JOURNAL OF VIROLOGY, Jan. 1986, p. 328–334
0022-538X/86/010328-07$02.00/0

Vol. 57, No. 1

# Coronavirus Minus-Strand RNA Synthesis and Effect of Cycloheximide on Coronavirus RNA Synthesis

STANLEY G. SAWICKI* AND DOROTHEA L. SAWICKI
*Department of Microbiology, Medical College of Ohio, Toledo, Ohio 43614*

Received 20 June 1985/Accepted 6 September 1985

**The temporal sequence of coronavirus plus-strand and minus-strand RNA synthesis was determined in 17CL1 cells infected with the A59 strain of mouse hepatitis virus (MHV). MHV-induced fusion was prevented by keeping the pH of the medium below pH 6.8. This had no effect on the MHV replication cycle, but gave 5- to 10-fold-greater titers of infectious virus and delayed the detachment of cells from the monolayer which permitted viral RNA synthesis to be studied conveniently until at least 10 h postinfection. Seven species of poly(A)-containing viral RNAs were synthesized at early and late times after infection, in nonequal but constant ratios. MHV minus-strand RNA synthesis was first detected at about 3 h after infection and was found exclusively in the viral replicative intermediates and was not detected in 60S single-stranded form in infected cells. Early in the replication cycle, from 45 to 65% of the [$^3$H]uridine pulse-labeled RF core of purified MHV replicative intermediates was in minus-strand RNA. The rate of minus-strand synthesis peaked at 5 to 6 h postinfection and then declined to about 20% of the maximum rate. The addition of cycloheximide before 3 h postinfection prevented viral RNA synthesis, whereas the addition of cycloheximide after viral RNA synthesis had begun resulted in the inhibition of viral RNA synthesis. The synthesis of both genome and subgenomic mRNAs and of viral minus strands required continued protein synthesis, and minus-strand RNA synthesis was three- to fourfold more sensitive to inhibition by cycloheximide than was plus-strand synthesis.**

Coronaviruses are enveloped RNA viruses that replicate in the cytoplasm of infected cells. The best-studied member is mouse hepatitis virus (MHV). Coronavirus assembly (9), molecular biology, and pathogenesis (23) have recently been reviewed. The coronaviruses possess a continuous plus-strand RNA genome of $5.4 \times 10^6$ to $6.9 \times 10^6$ daltons that is capped at its 5′ end and contains a poly(A) sequence at its 3′ end (12, 13, 22, 27). Coronaviruses resemble two other families of plus-strand RNA viruses, the picornaviruses and the alphaviruses, in their intracellular synthesis of virus-encoded, RNA-dependent RNA polymerases (5, 8), which are not found in the virion-associated form (7).

The coronavirus plus-strand genome serves as a template for the synthesis of a negative-strand RNA (12), which then serves as a template for transcription of progeny genome RNA and, depending on whether the virus is an avian or mammalian coronavirus, for transcription of five or six subgenomic mRNAs (25–27, 30). The subgenomic mRNAs form a nested set of molecules which are 3′ coterminal (6, 27, 31). Several models (11, 24) for transcription of these mRNAs have been proposed to explain the findings that the UV target size is proportional to the length of each mRNA (10) and that there is present in each mRNA a common 5′ leader sequence (12, 26).

We determined the temporal sequence and protein synthesis requirements for the synthesis of coronavirus plus-strand and minus-strand RNA. Brayton et al. (5) reported that only minus-strand synthesis was detectable in vitro with extracts of MHV (strain A59)-infected cells harvested at 1 h postinfection (p.i.), and only plus-strand synthesis was detectable in extracts of cells harvested at 6 h p.i. They concluded that coronavirus minus-strand synthesis was temporally distinct from that of plus-strand synthesis. If confirmed, this pattern would be unique among the plus-strand viruses.

* Corresponding author.

## MATERIALS AND METHODS

**Cells and virus.** Seventeen clone one (17CL1) mouse cells and the A59 strain of MHV (28) were kindly provided by Lawrence S. Sturman. 17CL1 cells were grown in Dulbecco modified Eagle medium containing 5% fetal bovine serum, 5% tryptose phosphate broth, 500 U of penicillin per ml, and 100 U of streptomycin per ml. MHV was twice plaque purified in 17CL1 cells and grown in 17CL1 cells. High-titer stocks of MHV were prepared by infecting confluent monolayers of 17CL1 cells with MHV diluted in pH 6.8 DMEM [Dulbecco modified Eagle medium containing 740 mg of sodium bicarbonate per liter, 10 mM *N*-1-hydroxyethylpiperazine-*N*′-2-ethanesulfonic acid, 10 mM 2-(*N*-morpholino)ethanesulfonic acid] containing 5% fetal bovine serum and 5% tryptose phosphate broth. The cells were not rinsed before infecting them. After an adsorption period of 1 h at 37°C, the inoculum was removed, and the cells were fed with pH 6.8 DMEM supplemented with 5% fetal bovine serum and 5% tryptose phosphate broth. One day after infection the supernatant was clarified by centrifugation at 10,000 × *g* for 10 min at 4°C and stored on ice or at −80°C. Titers were determined by plaque assay on monolayers of 17CL1 cells in 60-mm petri dishes overlaid with medium containing 0.1% Gelrite (Kelco, San Diego, Calif.). Titers of $5 \times 10^8$ PFU/ml were routinely obtained.

**Radiolabeling and isolation of MHV RNA.** 17CL1 cells in 35-, 60-, or 100-mm petri dishes were infected with MHV as described above with a multiplicity of infection of 50 to 100 PFU per cell. After the adsorption period, the infected cells were fed with pH 6.8 DMEM supplemented with 5% fetal bovine serum. The cells were fed with medium that contained 2 μg of actinomycin D (a generous gift of Merck Sharp & Dohme, West Point, Pa.) per ml 1 or 2 h before labeling with [$^3$H]uridine (34 Ci/mmole; ICN Radiochemicals, Irvine, Calif.) in the continued presence of actinomycin D. At the end of the labeling period, the [$^3$H]uridine-containing medium was removed, the monolayer was washed with phos-

phate-buffered saline, and the cells were solubilized in a small volume of NET buffer (0.1 M NaCl, 0.001 M EDTA, and 0.01 M Tris hydrochloride, pH 7.2) containing 5% sodium dodecyl sulfate. The solubilized cell extracts were passed through a 21-gauge needle and layered onto 15 to 30% sucrose gradients and centrifuged at 20°C in an SW27 rotor at 20,000 rpm for 16 h, which pelleted the 60S viral RNA, or for 12 h, which placed the 60S viral RNA one-third from the bottom of the tube. Alternatively, the solubilized cells were deproteinized by extraction with 2 volumes of phenol followed by 2 volumes of chloroform.

**Chromatography on sepharose 2B and CF-11 cellulose.** The viral RNA was separated according to size by chromatography on Sepharose 2B columns (1.5 by 90 cm; Pharmacia, Uppsala, Sweden) as previously described (19). Before chromatography the extracted RNA was treated with 10 μg of DNase (RNase free; Bethesda Research Laboratories, Inc., Gaithersburg, Md.) per ml in 50 mM sodium acetate (pH 6.5)–10 mM $MgCl_2$–2 mM $CaCl_2$ for 30 min at 37°C, followed by the addition of EDTA to 50 mM and sodium dodecyl sulfate to a final concentration of 1%. Viral replicative intermediate (RI) and replicative form (RF) eluted in the void volume and was collected by ethanol precipitation in the presence of unlabeled carrier tRNA.

Chromatography of viral RIs and RFs on CF-11 cellulose columns (Whatman, Inc., Clifton, N.J.) has been described before (21). Briefly, columns of CF-11 cellulose in 3-ml plastic syringes (2.5 ml of CF-11 cellulose) were extensively washed with STE buffer (0.1 M NaCl, 0.05 M Tris hydrochloride [pH 6.8], 10 mM EDTA) containing 1% beta-mercaptoethanol followed by 35% ethanol–STE buffer. After application of the RNA sample, which had been adjusted to 35% ethanol in STE buffer, the columns were washed sequentially with 35% ethanol–STE (15 ml) and with 15% ethanol–STE (15 ml) before elution of the RF RNA with STE buffer alone (9 ml). The RF RNA was ethanol precipitated in the presence of 25 μg of carrier tRNA. Viral RIs which had been obtained by chromatography of cell extracts on Sepharose 2B, were treated with 0.02 or 0.4 μg of RNase A per ml at 25°C for 15 min in 0.15 M NaCl–0.01 M Tris hydrochloride (pH 7.4) before being chromatographed on CF-11 cellulose. Determination of the amount of alkali-resistant radioactivity in RNA preparations employed incubation of the samples at 37°C for 16 h in 0.3 M KOH and collection on filters of the acid-insoluble radioactivity.

**Determination of MHV minus-strand RNA synthesis.** The procedures used for measuring MHV minus-strand RNA were similar to those described for detection of alphavirus minus-strand synthesis (20, 21). Purified, unlabeled, virion plus-strand RNA was dissolved after ethanol precipitation in 1 mM EDTA at a concentration of 1 mg/ml (25 units of absorbancy at 260 nm per mg) and stored at −20°C in small samples. Viral RF RNA was obtained either as described above or from infected cell RNA which had been extracted with phenol and chloroform, treated with RNase A, and chromatographed twice on CF-11 cellulose. Hybridization of the RF RNA, which was denatured by heating at 100°C for 3 to 5 min followed by quick cooling at 0°C, was at 68 to 70°C for 30 min, followed by an incubation of 30 min at 25°C. The annealing reaction employed 10 μg of unlabeled purified virion plus-strand RNA and was performed in a final volume of 1 ml of 0.4 M NaCl–1 mM EDTA.

## RESULTS

The time course of viral RNA synthesis of 17CL1 cells infected with 100 PFU of the A59 strain of MHV per cell is shown in Fig. 1. Before 3 h p.i., viral RNA synthesis could not be detected above the level of incorporation of [$^3$H]uridine observed in mock-infected 17CL1 cells. Beginning at about 3 h p.i., the rate of viral RNA synthesis increased until about 5 h p.i. Decreasing the multiplicity of infection to 5 PFU/cell delayed by about 1 h the time at which viral RNA synthesis was first observed. At about 6 h p.i., cell fusion began to occur, and by 8 to 9 h p.i. the giant, multinuclear cells were sloughed from the monolayer. We found that we could prevent MHV-induced cell fusion by maintaining the pH of the culture medium below neutrality. This was accomplished by using one-fifth of the regular concentration of sodium bicarbonate in Dulbecco modified minimum essential medium and keeping the $CO_2$ level at 10%. The data presented in Fig. 1 demonstrate that lowering the pH did not affect viral RNA synthesis in 17CL1 cells, but did extend the time during which viral RNA synthesis could be conveniently assayed. Under conditions of lowered pH, the rate of viral RNA synthesis during the late period remained approximately constant (Fig. 1). The rate of viral RNA synthesis in infected cells maintained in pH 7.2 medium was the same as in pH 6.8 medium until about 8 h p.i., when the rate of viral RNA synthesis declined (Fig. 1). The production of infectious virus did not appear to be affected by preventing MHV-induced cell fusion and occurred at the same time in pH 6.8 medium as it did in pH 7.2 medium. However, infected cells maintained at pH 6.8 continued to

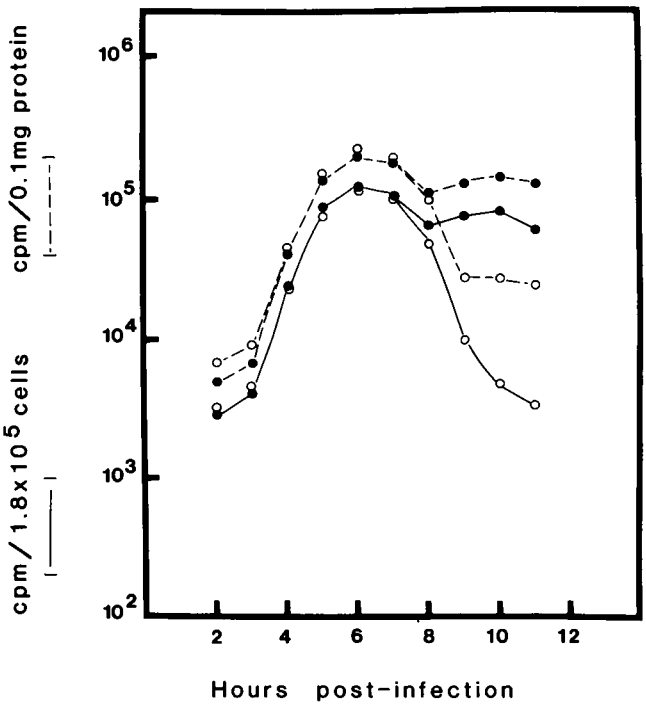


FIG. 1. Time course of MHV RNA synthesis at pH 7.2 or 6.8. Cultures of 17CL1 cells in 35-mm petri dishes were infected with MHV (multiplicity of infection of 100) and maintained at 37°C in medium at pH 7.2 (○) or at pH 6.8 (●) as described in Materials and Methods. The cultures were labeled with [$^3$H]uridine for 60-min periods between 1 and 11 h p.i., and the cells were solubilized in NET buffer with sodium dodecyl sulfate. The acid-insoluble radioactivity in 1/10 of the sample was determined (——). The protein content in 1/10 of each sample was determined by the method of Lowry et al. (15), and the acid insoluble radioactivity expressed per 0.1 mg of protein (-----).

release MHV for a longer time and produced higher titers of MHV than did cells maintained at pH 7.2. Thus, MHV resembles avian infectious bronchitis (1) and transmissible gastroenteritis (18) viruses in their ability to grow to higher titers at low pH. The results which follow were obtained with low-pH conditions.

We determined the relative proportion of synthesis of the viral genome RNA and the subgenomic mRNA species during different periods of the MHV replication cycle. Similar to the results published by Leibowitz et al. (14), we found seven species of MHV RNA by acid-urea-agarose gel or by formaldehyde-agarose electrophoresis of oligo (dT) cellulose-selectable RNA or total RNA from MHV-infected cells that had been pulse-labeled with $^{32}P_i$ or with [$^3$H]uridine (data not shown). No incorporation of [$^3$H]uridine into 60S genomic or subgenomic RNA was detected before 2 to 3 h p.i. In our laboratory the A59 strain of MHV synthesized approximately as much 60S RNA on a weight basis as subgenomic RNA.

We next determined when minus-strand RNA was synthesized in the MHV replication cycle. Because of the report by Brayton et al. (5), we were especially careful to look for minus-strand RNA synthesis early in the infection. MHV-infected cells were pulse-labeled with [$^3$H]uridine for 1-h periods between 1 and 8 h p.i. The total cell extract was analyzed by rate zonal centrifugation on sucrose gradients. The radiolabeled RNA sedimenting at 60S was collected by ethanol precipitation, and the 60S RNA was allowed to anneal to an excess of unlabeled virion plus strands. Less than 1% of the radiolabeled RNA sedimenting at 60S was protected from RNase A digestion (Table 1). However, when purified viral RF RNA obtained from MHV-infected cells labeled with [$^3$H]uridine from 2.5 to 6 h p.i. (see below) was denatured and annealed under identical conditions, 45% of the radiolabel was protected from RNase A digestion (data not shown). We conclude that at no time in the infectious cycle did MHV-infected cells contain significant amounts of genome-length, single-stranded, minus-strand RNA. Therefore, purification and analysis of the viral double-stranded RIs was undertaken to determine the kinetics of viral minus-strand synthesis.

We found that cells infected with our stocks of MHV synthesized large amounts of genome-sized 60S RNA, and that this RNA coeluted with the viral RIs in the void volume fractions of Sepharose 2B, Sepharose 2B-CL, or Ultrogel A2 columns (data not shown). Therefore, to separate the 60S single-strand RNA from the partially double-stranded viral RIs and to obtain an enrichment of the viral RIs, we first fractionated the intracellular viral RNA species by sucrose gradient centrifugation and pooled the region of the gradient containing the RIs. Figure 2 shows a formaldehyde-agarose gel of various fractions of a sucrose gradient of $^{32}$P-labeled, MHV-infected cell extracts. Fraction 37 was the top, and fraction 1 was the bottom, of the gradient. The viral RIs and RFs were identified as RNase A-resistant radioactivity and were found to sediment between 40 and 10S (fractions 15 to 30 in Fig. 2). We then routinely used conditions of sedimentation that resulted in the pelleting of the 60S RNA and that clearly separated the RI region from the 60S RNA. When infected cultures were pulsed for 5 min with [$^3$H]uridine at 6 h p.i., 38% of the labeled RNA that sedimented between 40 and 10S was found to elute in the void volume of Sepharose 2B columns (data not shown); 52% of this labeled RNA was resistant to digestion with RNase A, but it was completely digestable with alkali. When rechromatographed, all of the labeled RNA was again recovered in the void volume. The 5-min pulse-labeled viral RIs sedimented heterogeneously on sucrose gradients, with a peak at about 26S, as reported previously by Baric et al. (2). Their behavior during chromatography on CF-11 cellulose was also consistent with that expected of an RI molecule: 40% of the labeled RNA eluted in the 15% ethanol–STE fraction, and 60% eluted in the STE fraction. However, pretreatment with low levels of RNase A (0.4 μg/ml) resulted in all of the labeled RNA eluting in the

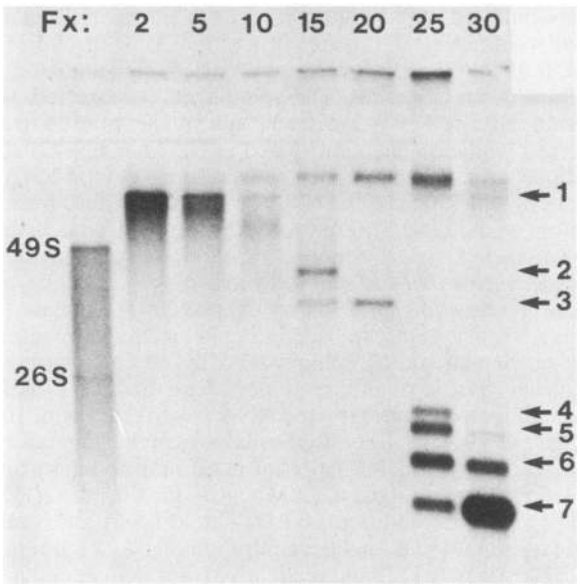


FIG. 2. Formaldehyde agarose gel electrophoresis of MHV RNA species. MHV-infected cells were labeled with 1 mCi of $^{32}$P per ml in phosphate-free medium for 1 h at 6 h p.i. in the presence of 10 μg of actinomycin D per ml. The cells were solubilized in NET buffer with 5% sodium dodecyl sulfate and layered onto 15 to 30% sucrose gradients in NET buffer containing 0.2% sodium dodecyl sulfate and centrifuged in an SW27 rotor at 20,000 rpm for 16 h at 20°C. The gradient was fractionated into 1-ml fractions. Small samples of fractions 2, 5, 10, 15, 20, 25, and 30 were diluted and made 50% formamide and 2.2 M formaldehyde, heated to 55°C for 15 min, and subjected to electrophoresis on 1% agarose gels in 2.2 M formaldehyde in 20 mM morpholinopropanesulfonic acid–5 mM sodium acetate–2 mM EDTA (pH 7.3). The first lane shows size markers of Semliki Forest virus 49S and 26S RNA.

TABLE 1. Absence of single-stranded 60S minus-strand RNA[a]

| Time p.i. (h) | 60S MHV RNA | | | | RF RNA (cpm) | |
|---|---|---|---|---|---|---|
| | Total (cpm) | Assayed (cpm) | Minus strand | | Total | Minus strand |
| | | | cpm | % | | |
| 1 to 2 | 5,183 | 1,024 | 4 | 0.5 | 0 | 0 |
| 2 to 3 | 1,741 | 485 | 0 | <0.1 | 0 | 0 |
| 3 to 4 | 15,438 | 2,328 | 21 | 1.0 | 0 | 0 |
| 4 to 5 | 163,402 | 2,747 | 21 | 0.8 | 455 | 189 |
| 5 to 6 | 423,332 | 6,887 | 14 | 0.2 | 868 | 385 |
| 7 to 8 | 245,042 | 7,111 | 9 | 0.2 | 1,575 | 132 |

[a] Cultures of 17CL1 cells in 60-mm petri dishes were infected at a multiplicity of infection of 100 with MHV strain A59 and were treated with actinomycin D (2 μg/ml) beginning at 1 h p.i. Pulses of 1 h were given with [$^3$H]uridine (200 μCi/ml) as described in Materials and Methods. The 60S RNA was recovered after rate zonal centrifugation on sucrose gradients; the RF RNA was obtained after RNase treatment of 40 to 10S RNA and chromatography on CF-11 cellulose. Hybridization was as described in Materials and Methods.

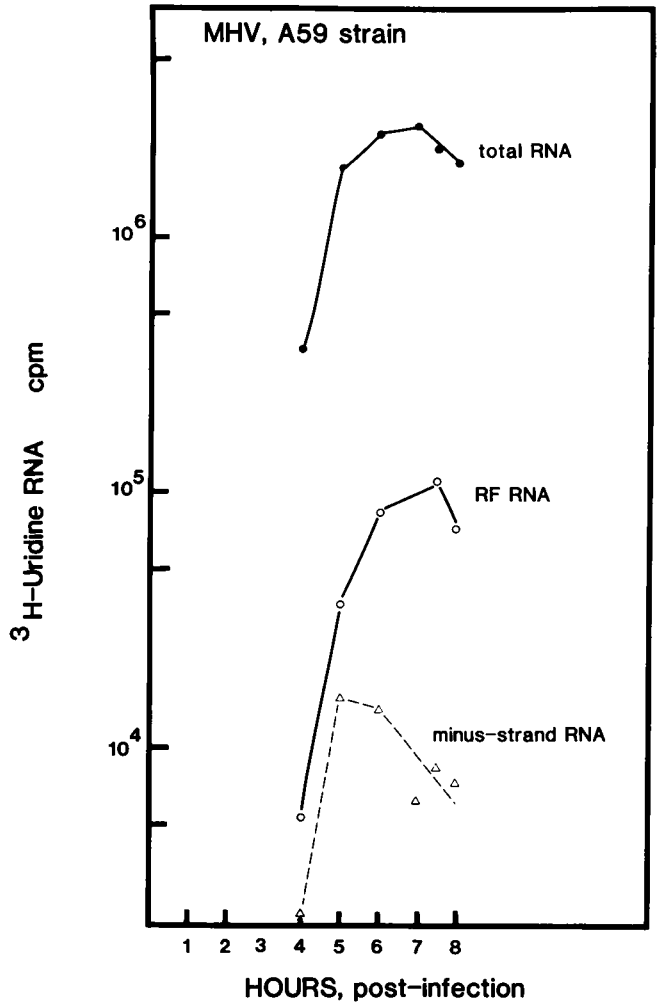


FIG. 3. Kinetics of MHV minus-strand and plus-strand RNA synthesis. Cultures of 17CL1 cells in 100-mm petri dishes were infected with MHV (multiplicity of infection of 100). The cultures were treated with actinomycin D (2 μg/ml) for 1 h before pulse-labeling with [$^3$H]uridine for 30 min starting at 3.5 h p.i. The viral RI RNA was obtained by sedimentation on linear 15 to 30% sucrose gradients and digested with RNase A. The RF RNA was obtained by chromatography on CF-11 cellulose, heat denatured, and annealed to an excess of unlabeled virion RNA as described in Materials and Methods. The [$^3$H]uridine-labeled RNA that was resistant to digestion with RNase A after hybridization was considered to be minus-strand RNA.

STE fraction, consistent with the formation of a completely double-stranded RF molecule. Under these conditions, DNA elutes in the 15% ethanol–STE fraction. By combining DNase treatment before Sepharose 2B chromatography and the use of CF-11 chromatography to further purify the viral double-stranded RNA from DNA and single-stranded RNA, we were able to isolate labeled minus strands as part of the viral RIs or RFs. MHV-infected cells were labeled with [$^3$H]uridine from 2.5 to 6 h p.i., and the 40 to 10S RNA was collected after sedimentation of infected cell extracts on sucrose gradients and subjected to chromatography on CF-11 cellulose. The labeled RFs represented about 1% of the labeled RNA in the original infected extracts. Samples of the purified RF RNA corresponding in amount to that present in about $3 \times 10^6$ cells were analyzed in hybridization assays with increasing amounts (1 to 50 μg/ml) of purified virion plus strands. Maximum amounts of hybridization (45 to 65% of the labeled RF RNA) were found when 5 μg or more of plus-strand RNA per ml was used in each assay. Since the labeling period encompassed essentially the entire period of minus-strand synthesis, approximately 50% of the total labeled RF RNA would be expected to be in minus-strand RNA. Having successfully isolated MHV RIs and RFs and detected viral minus-strand RNA in the amounts expected, we next determined the kinetics of MHV minus-strand synthesis.

Figure 3 presents the results of our investigation on the kinetics of MHV minus-strand and plus-strand RNA synthesis. Infected cultures were pulsed with [$^3$H]uridine for 30-min periods between 3 and 8 h p.i. The viral RF RNA (1.4 to 3% of the total labeled viral RNA) was isolated by chromatography on CF-11 cellulose. Beginning at about 3 h p.i., the rate of incorporation of radiolabel into RF RNA began to increase, and it paralleled the increase in the rate of overall viral RNA synthesis. Minus-strand RNA synthesis was detectable at 3 h p.i. and increased in proportion to the labeling of RF RNA. The overall rates of viral RNA synthesis (the vast majority of which was plus-strand RNA), of accumulation of RF RNA, and of minus-strand synthesis reached a maximum at about 6 h p.i. The rate of minus-strand synthesis declined after 6 h p.i. to about 20% of the maximum rate.

We next asked whether coronavirus RNA synthesis required continued protein synthesis. The effect of adding cycloheximide at different times after infection on the rate of synthesis of MHV RNA is shown in Fig. 4. Inhibition of protein synthesis before 3 h p.i. prevented MHV RNA synthesis, whereas inhibition of protein synthesis after 3 h p.i. prevented the rate of MHV RNA synthesis from increas-

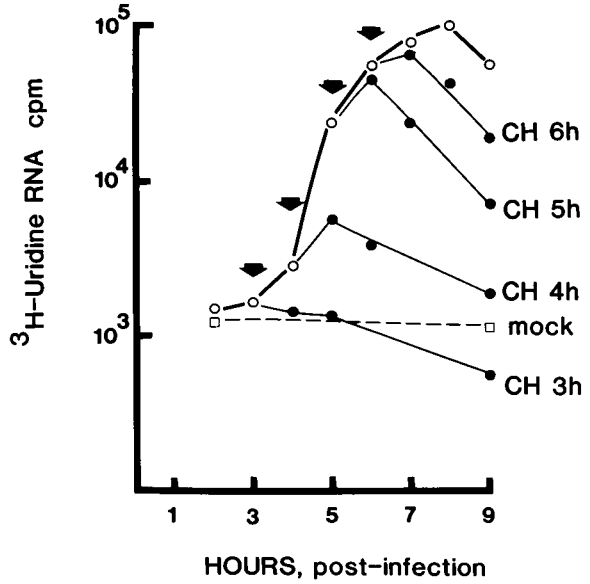


FIG. 4. Effect of cycloheximide (CH) on MHV RNA synthesis. 17CL1 cells in 35-mm petri dishes ($2.5 \times 10^6$ cells per dish) were infected with MHV (multiplicity of infection of 100). The cultures were pulse labeled with [$^3$H]uridine (100 μCi/ml) for 60 min (○) in the presence of actinomycin D (20 μg/ml). At 3, 4, 5, and 6 h p.i. (arrows), cycloheximide at 100 μg/ml was added to sets of three cultures. Each set of infected cultures was labeled for 60 min with [$^3$H]uridine in the presence of actinomycin D and cycloheximide at the times indicated (●).

ing. To determine whether the synthesis of the MHV genomic 60S RNA was differentially sensitive to inhibition of protein synthesis compared with the viral subgenomic mRNA, infected cultures were treated with cycloheximide beginning at 5 h p.i. and pulsed with [$^3$H]uridine for 60-min periods in the presence of cycloheximide between 5 and 7 h p.i. Extracts of the infected cells were analyzed by formaldehyde-agarose gel electrophoresis (Fig. 5). Both the 60S RNA and the subgenomic mRNA species were produced in untreated cultures. With increased time of cycloheximide treatment, diminished incorporation of radiolabel into all viral plus-strand RNA species was found. There was an approximately 50% reduction in the overall rate of RNA synthesis for every 30 min of cycloheximide treatment. This reduction was not due to the loss of cells from the monolayers, since equal amounts of rRNA were present in extracts of cells treated or not treated with cycloheximide. The synthesis of all species of MHV mRNA was found to decrease proportionally with increasing time of cycloheximide treatment (Fig. 6). Thus, all species of MHV plus strands appeared to be equally sensitive to inhibition by the protein synthesis inhibitor.

The cycloheximide-treated cultures were also analyzed for their ability to continue minus-strand synthesis in the absence of continued protein synthesis. Cultures were infected with MHV and were incubated at 37°C until 5 h p.i., when cycloheximide was added to one-half of the cultures. Pulses of [$^3$H]uridine were given for 30-min periods between 4.5 and 6 h p.i. to the untreated cultures and between 5 and 6.5 h p.i. to the cycloheximide-treated cultures (Fig. 6). The rate of synthesis of MHV 60S and 16S (RNA 4, 5, 6, 7) plus-strand RNA declined at a linear rate with increasing time of cycloheximide treatment, but continued to be synthesized at a relatively constant rate in the absence of the protein synthesis inhibitor (Fig. 6A). Moreover (Fig. 6B), coronavirus minus-strand synthesis was inhibited by cycloheximide treatment, and its synthesis appeared to be at least three times more sensitive than was plus-strand RNA synthesis. We conclude that both coronavirus plus- and minus-strand synthesis required continued protein synthesis.

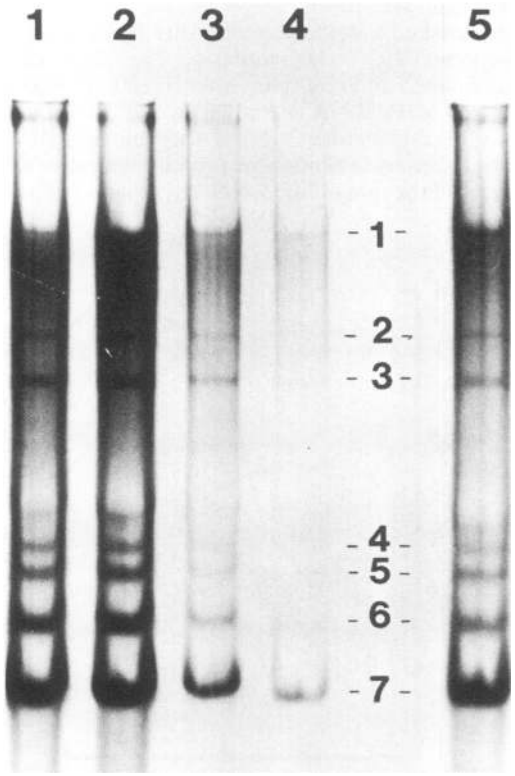


FIG. 5. Cycloheximide sensitivity of MHV plus-strand RNA synthesis. MHV-infected cells were treated with 100 μg of cycloheximide per ml at 5 h p.i. and labeled with [$^3$H]uridine (100 μCi/ml) for 1 h at 5 (lanes 1 and 3) and 6 (lanes 2, 4 and 5) h p.i. in the presence (lanes 3, 4, and 5) or absence (lanes 1 and 2) of cycloheximide. The cells were solubilized in NET buffer containing 5% sodium dodecyl sulfate and extracted twice with phenol and twice with chloroform. The RNA was ethanol precipitated, denatured with 50% formamide–2.2 M formaldehyde at 55°C for 15 min, and electrophoresed on 1% agarose gels containing 2.2 M formaldehyde. Lane 5 is the same as lane 4, except the exposure was four times longer.

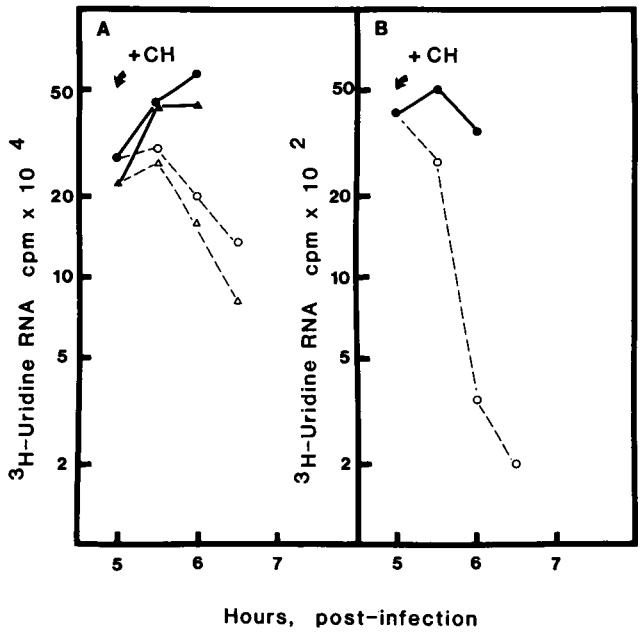


FIG. 6. Comparison of the cycloheximide sensitivity of MHV minus-strand and plus-strand RNA synthesis. Cultures of 17CL1 cells were infected with MHV as described in Materials and Methods. Cycloheximide (100 μg/ml) was added to three cultures beginning at 5 h p.i. The cultures were labeled with [$^3$H]uridine (200 μCi/ml) for 30 min between 5 and 6.5 h p.i. The viral RNA was resolved on 15 to 30% sucrose gradients. A, Incorporation obtained in the 60S (△, ▲) and the 16S (○, ●) regions of the gradients in untreated (——) and cycloheximide-treated (-----) cultures. B, Incorporation of [$^3$H]uridine into minus strands was determined as described in the legend to Fig. 3 and in Materials and Methods for untreated (●) and cycloheximide-treated (○) cultures.

## DISCUSSION

The results of our studies on MHV indicated that the synthesis of both plus- and minus-strand RNA was first detected beginning at about 3 h p.i. at 37°C. The synthesis of both plus- and minus-strand RNA was observed to increase between 3 and 5 h p.i. The increase in the number of minus strands led to the accumulation of increased numbers of viral RIs which were mostly engaged in plus-strand RNA synthesis. At all times investigated, the synthesis of 60S genome RNA was proportional in total incorporation to that of the most prominent subgenomic mRNA, the 16S mRNA or

mRNA 7. Since there is an approximate 10-fold difference in the molecular weight of the 60S genome RNA and the 16S mRNA (14), cells infected with our strain of MHV synthesized 10 times more 16S mRNA than genome RNA and thus synthesized 3 to 4 times more genome RNA than that reported by Leibowitz et al. (14). The pattern of overall MHV RNA synthesis was identical to that reported by others, who found that the synthesis of viral mRNA species first became detectable at 4 h p.i. with agarose gel electrophoresis (14). Our results also agree with those of Stern and Kennedy (27), Wege et al. (30), Spaan et al. (25), and Leibowitz et al. (14) in finding a nonequimolar synthesis of the seven viral mRNA species at all times during the replication cycle.

Viral RIs contained essentially all of the viral minus-strand RNA. No single-stranded 60S minus-strand RNA was detected in infected cell extracts at immediate early, early, or late periods in the viral replication cycle. Our failure to find single-stranded 60S minus-strand RNA early in infection is not in agreement with the suggestion of Brayton et al. (5) that there is an early time when only minus-strand RNA is synthesized. In the absence of viral plus strands, there should be free, single-stranded minus-strand RNA molecules if they were synthesized in amounts sufficient to be detected and if they were 60S in size. If, on the other hand, MHV minus-strand polymerase was formed but not active in vivo at immediate early times, its activity might be detectable in vitro. Our studies on the temporal appearance of viral plus-strand and minus-strand RNA are in agreement with the results of Dennis and Brian (7, 8) on the temporal appearance of viral RNA synthesis in porcine transmissible gastroenteritis virus-infected cells.

The synthesis of MHV minus-strand RNA was readily detectable by 4 h p.i., at about the same time that plus-strand synthesis was detectable. The proportion of [$^3$H]uridine incorporated into minus strands relative to plus strands in the RF RNA remained at 40 to 50% during the early period of the viral replication cycle, when the rate of plus-strand RNA synthesis was increasing exponentially (four- to eightfold every 30 min). Because the rate of minus-strand RNA synthesis was also increasing exponentially, pulse labels of 30 min or longer would result in the majority of minus strands becoming labeled during the pulse period. Hence, even though minus strands, unlike plus strands, remained in the RIs and were not released as single-stranded species after their synthesis, the relative numbers of minus strands that were synthesized during the pulse period must have exceeded the number of minus-strand templates that were synthesized before the pulse period. The synthesis of minus strands was followed by accumulation of increased incorporation of radiolabel into replicative intermediates. However, the synthesis of minus strands declined after 6 h p.i., the same time that the overall rate of plus-strand synthesis and of incorporation of [$^3$H]uridine into viral RIs became constant. This pattern is similar to that of alphaviruses (20). Because plus-strand synthesis continued after the synthesis of minus-strand RNA had significantly decreased and because the incorporation of [$^3$H]uridine into viral RIs remained relatively constant, we conclude that the viral minus strands are stable and function as templates for a long time after their synthesis. Although there was a significant decrease in the rate of viral minus-strand synthesis in MHV-infected cells, it did not decrease to the very low levels observed during the late period in alphavirus-infected cells (20).

The synthesis of both plus-strand and minus-strand RNA in MHV-infected cells required continued protein synthesis. This was clearly different from the requirements for newly synthesized proteins for continued synthesis of minus strands but not of plus strands, during alphavirus replication (20, 21). The decrease of MHV minus-strand synthesis after the addition of cycloheximide was three to four times greater than the decrease of plus-strand synthesis. Also, the decrease in the rate of plus-strand synthesis after the addition of cycloheximide occurred only after 20 to 30 min, whereas minus-strand synthesis was more immediately affected. Minus strands were minor species in MHV-infected cells, accounting for 2% or less of the total incorporation of radiolabel into viral RNA. Thus, because there may be only a few RIs active in minus-strand synthesis, a decrease in their function might be more readily apparent. Alternatively, there may be a greater sensitivity of the minus-strand polymerase activity than of the plus-strand polymerase activity to protein synthesis inhibition. The synthesis of both genome 60S RNA and the subgenomic mRNAs appeared to be equally sensitive to inhibition of protein synthesis. Thus, coronavirus plus-strand synthesis appears to utilize a mechanism that also differs from that used by the negative-stranded RNA rhabdoviruses. The replication of genome-sized plus- and minus-strand RNA by the rhabdovirus vesicular stomatitis virus required continued synthesis of viral nucleocapsid protein (3, 4, 16, 32), but the transcription of viral mRNA by these cells did not require continued protein synthesis (17, 33).

The sensitivity of coronavirus RNA synthesis to cycloheximide more closely resembled that seen for poliovirus RNA synthesis. It has been suggested that the failure to synthesize the polyprotein precursor to the VPg leads to the rapid inhibition of poliovirus RNA synthesis (29). Therefore, the poliovirus replicase may function for one round of synthesis and require newly synthesized viral polypeptides to initiate each round of viral RNA synthesis. Coronavirus transcription may involve a viral polymerase that is either turned over or short lived or may require a newly synthesized viral protein to initiate viral RNA synthesis. The presence of the 5′ cap structure on coronavirus plus-strand RNA species (12) argues against a function for a VPg-like polypeptide in coronavirus plus-strand RNA synthesis. Since the mechanisms hypothesized for coronavirus mRNA synthesis involve the synthesis of a leader sequence and its movement to a region adjacent to the start of the respective mRNA coding sequence in the template RNA (2), continued synthesis of a protein that functions in specific initiation or translocation may be required for coronavirus transcription.

## ACKNOWLEDGMENTS

We especially thank Lawrence S. Sturman for his encouragement and generous provision of virus and cells and K. V. Holmes for advice. Debora Bruner provided excellent technical assistance, and Cheryl Zimmerman typed the manuscript.

This investigation was supported by the United States-Japan Medical Sciences Program through Public Health Service grant AI-15123 from the National Institutes of Health and by Public Health Service Research Career Development Award AI-00510 (to D.L.S.) from the National Institutes of Health.

## LITERATURE CITED

1. **Alexander, D. J., and M. S. Collins.** 1975. Effect of pH on the growth and cytopathogenicity of avian infectious bronchitis virus in chick kidney cells. Arch. Virol. **49**:339–348.
2. **Baric, R. S., S. A. Stohlman, and M. M. C. Lai.** 1983. Characterization of replicative intermediate RNA of murine hepatitis virus: presence of leader RNA sequences on nascent chains. J.

Virol. **48**:633–640.
3. **Blumberg, B. M., C. Giorgi, and D. Kolakofsky.** 1983. N Protein of vesicular stomatitis virus selectively encapsidates leader RNA in vitro. Cell **32**:559–567.
4. **Blumberg, B. M., M. Leppert, and D. Kolakofsky.** 1981. Interaction of leader RNA and nucleocapsid protein may control VSV genome replication. Cell **23**:837–845.
5. **Brayton, P. R., M. M. C. Lai, C. D. Patton, and S. A. Stohlman.** 1982. Characterization of two RNA polymerase activities induced by mouse hepatitis virus. J. Virol. **42**:847–853.
6. **Cheley, S., R. Anderson, M. J. Cupples, E. C. M. Leechan, and V. L. Morris.** 1981. Intracellular murine hepatitis virus-specific RNAs contain common sequences. Virology **112**:596–604.
7. **Dennis, D. E., and D. A. Brian.** 1981. Coronavirus cell-associated RNA-dependent RNA polymerase. Adv. Exp. Biol. Med. **142**:155–170.
8. **Dennis, D. E., and D. A. Brian.** 1982. RNA-dependent RNA polymerase activity in coronavirus-infected cells. J. Virol. **42**:153–164.
9. **Dubois-Dalcq, M., K. V. Holmes, and B. Rentier.** 1984. Assembly of coronaviridae, p. 100–119. *In* Assembly of enveloped viruses. Springer-Verlag, New York.
10. **Jacobs, L., W. J. M. Spaan, M. C. Horzinek, and B. A. M. van der Zeijst.** 1981. Synthesis of subgenomic mRNAs of mouse hepatitis virus is initiated independently: evidence from UV transcription mapping. J. Virol. **39**:401–406.
11. **Lai, M. M. C., C. D. Patton, R. S. Baric, and S. A. Stohlman.** 1983. Presence of leader sequences in the mRNA of mouse hepatitis virus. J. Virol. **46**:1027–1033.
12. **Lai, M. M. C., D. C. Patton, and S. A. Stohlman.** 1982. Replication of mouse hepatitis virus: negative-stranded RNA and replicative form are of genome length. J. Virol. **44**:487–492.
13. **Lai, M. M. C., and S. A. Stohlman.** 1978. RNA of mouse hepatitis virus. J. Virol. **26**:236–242.
14. **Leibowitz, J. L., and K. C. Wilhemsen, and C. W. Bond.** 1981. The virus specific intracellular species of two murine coronaviruses: MHV-A59 and MHV-JHM. Virology **114**:39–51.
15. **Lowry, O. H., N. J. Rosebrough, A. L. Farr, and R. J. Randall.** 1951. Protein measurement with the Folin phenol reagent. J. Biol. Chem. **193**:265–275.
16. **Peluso, R. W., and S. A. Moyer.** 1984. Vesicular stomatitis virus proteins required for the *in vitro* replication of defective interfering particle genome RNA, p. 153–160. *In* D. H. L. Bishop and R. W. Compans (ed), Nonsegmented negative strand viruses. Academic Press, Inc., New York.
17. **Perlman, S. M., and A. S. Huang.** 1973. RNA synthesis of vesicular stomatitis virus. V. Interactions between transcription and replication. J. Virol. 12:1395–1400.
18. **Pocock, D. H., and D. J. Grawes.** 1975. The influence of pH on the growth and stability of transmissible gastroenteritis virus *in vitro*. Arch. Virol. **49**:239–247.
19. **Sawicki, D. L., and P. J. Gomatos.** 1976. Replication of Semliki Forest virus: polyadenylate in plus-strand RNA and polyuridylate in minus-strand RNA. J. Virol. **20**:446–464.
20. **Sawicki, D. L., and S. G. Sawicki.** 1980. Short-lived minus-strand polymerase for Semliki Forest virus. J. Virol. **34**:108–118.
21. **Sawicki, S. G., D. L. Sawicki, L. Kääriäinen, and S. Keränen.** 1981. A Sindbis virus mutant temperature sensitive in the regulation of minus-strand RNA synthesis. Virology **115**: 161–172.
22. **Siddell, S., H. Wege, and V. ter Meulen.** 1982. The structure and replication of coronaviruses. Curr. Top. Microbiol. Immunol. **99**:131–163.
23. **Siddell, S., H. Wege, and V. ter Meulen.** 1983. The biology of coronaviruses. J. Gen. Virol. **64**:761–776.
24. **Spaan, W., H. Delius, M. A. Skinner, J. Armstrong, P. Rottier, S. Smeekens, S. G. Siddell, and B. van der Zeijst.** 1983. Transcription strategy of coronaviruses: fusion of non-contiguous sequences during mRNA synthesis. Adv. Exp. Biol. **173**:173–186.
25. **Spaan, W. J. M., P. J. M. Rottier, M. C. Horzinek, and B. A. M. van der Zeijst.** 1981. Isolation and identification of virus-specific mRNAs in cells infected with mouse hepatitis (MHV-A59). Virology **108**:424–434.
26. **Spaan, W. J. M., P. J. M. Rottier, M. C. Horzinek, and B. A. M. van der Zeijst.** 1982. Sequence relationships between the genome and the intracellular RNA species 1, 3, 6, and 7 of mouse hepatitis virus strain A59. J. Virol. **42**:432–439.
27. **Stern, D. F., and S. I. T. Kennedy.** 1980. Coronavirus multiplication strategy. II. Mapping the avian infectious bronchitis virus intracellular RNA species to the genome. J. Virol. **36**:440–449.
28. **Sturman, L. S., and K. Takemoto.** 1972. Enhanced growth of a murine coronavirus in transformed mouse cells. Infect. Immun. **6**:501–507.
29. **Takegami, T., R. J. Kuhn, C. W. Anderson, and E. Wimmer.** 1983. Membrane-dependent uridylylation of the genome-linked protein VPg of poliovirus. Proc. Natl. Acad. Sci. USA **80**:7447–7451.
30. **Wege, H., S. G. Siddell, L. S. Sturman, and V. ter Meulen.** 1981. Coronavirus JHM: Characterization of intracellular viral RNA. J. Gen. Virol. **54**:213–217.
31. **Weiss, S. R., and J. L. Leibowitz.** 1983. Characterization of murine coronavirus RNA by hybridization with virus-specific cDNA probes. J. Gen. Virol. **64**:127–133.
32. **Wertz, G. W.** 1983. Replication of vesicular stomatitis virus defective interfering particle RNA in vitro: transition from synthesis of defective interfering leader RNA to synthesis of full-length defective interfering RNA. J. Virol. **46**:513–522.
33. **Wertz, G. W., and M. Levine.** 1973. RNA synthesis by vesicular stomatitis virus and a small plaque mutant: effects of cycloheximide. J. Virol. **12**:253–264.